# Proceedings of
# the 18th Japan-Taiwan International Workshop on Hydrological and Geochemical Research for Earthquake Prediction

3 September, 2018
GSJ, AIST, Tsukuba, Japan

Norio Matsumoto and Chjeng-Lun Shieh eds.

Disaster Prevention Research Center
National Cheng Kung University
No.1,Ta-Hsueh Rd. Tainan 701, Taiwan

IEVG
Research Institute of Earthquake and Volcano Geology
GEOLOGICAL SURVEY OF JAPAN
NATIONAL INSTITUTE OF
ADVANCED INDUSTRIAL SCIENCE AND TECHNOLOGY (AIST)
1-1 Higashi 1-Chome, Tsukuba, Ibaraki, 305-8567 Japan
2019

The 18th Japan-Taiwan International Workshop on Hydrological and Geochemical Research for Earthquake Prediction

3 September, 2019

Meeting room No.2, GSJ, AIST, Tsukuba, Japan

revised 2 Sep 2019

| No | From | To | Name | Presentation |
|---|---|---|---|---|
| Morning sesson | | | | |
| | 10:00 | 10:10 | Masahiko Makino (Assitant Director General, GSJ, AIST) | Greeting |
| 1 | 10:10 | 10:35 | Mamoru Nakamura (UR) | Seismicity Activation by Strain Rate Change in Iriomote Island, South Ryukyu |
| 2 | 10:35 | 11:00 | Yuzo Ishikawa (AIST) | M6.7 earthquake off Yamagata prefecture |
| 3 | 11:00 | 11:25 | Suguru Yabe (AIST) | Seismic energy estimation for shallow tremors in the Nankai trough |
| | 11:25 | 11:45 | Coffee break | |
| 4 | 11:45 | 12:10 | Kuo-Fong Ma (NCU) | Evolution of the seismic anisotropy associated with fluid and earthquakes through borehole observation |
| 5 | 12:10 | 12:35 | Ryoya Ikuta (SU) | Seismic velocity monitoring using ACROSS on landslide area |
| | 12:35 | 12:50 | Group Photo at the 1st floor of the building | |
| | 12:50 | 13:50 | Lunch (Lunch Meeting for presenters at Meeting Room No.1 at 8th floor) | |
| Afternoon session #1 | | | | |
| 6 | 13:50 | 14:15 | Min-Chien Tsai (CWB) | Assessment of seismic potential in Metropolitan Manila induced by the Marikina Valley fault: Insight from 2019 Castillejobs Mw 6.1 Earthquake |
| 7 | 14:15 | 14:40 | Jyr-Ching Hu (NTU) | Shallow coseismic slip in a triangle zone of 2019 ML 6.0 Changning earthquake in Sichuan Basin: Triggering by shale gas hydraulic fracturing? |
| 8 | 14:40 | 15:05 | Kuniyo Kawabata (KU) | 222Rn concentration distribution on active faults in Yatsushiro Sea |
| 9 | 15:05 | 15:30 | Ching-Chou Fu (IES, AS) | Exploring the release of radioactive gas in the volcanic area and its tectonic implications |
| | 15:30 | 15:50 | Coffee break | |
| Afternoon session #2 | | | | |
| 10 | 15:50 | 16:15 | Shih-Jung Wang (NCU) | Hydrology Anomalies Triggered by 2016 Taiwan Meinong Earthquake |
| 11 | 16:15 | 16:40 | Naoji Koizumi (USP) | Postseismic hydrological changes associated with the 2016 Kumamoto earthquake |
| 12 | 16:40 | 17:05 | Wen-Chi Lai (DPRC, NCU) | The study of the mechanism of earthquake-induced groundwater changes in Taiwan: An update in recent earthquakes |
| 13 | 17:05 | 17:30 | Norio Matsumoto (AIST) | Changes in groundwater pressure associated with the 2018 Osaka Hokubu earthquake (M6.1) at the Takarazuka observatory |
| | 17:30 | 18:00 | | Discussion |
| | 18:00 | | | Banquet (AIST Restrant, 2nd floor at the central bulding) |

RU: University of the Ryukyus
IES, AS: Institute of Earth Sciences, Academia Sinica, Taiwan
NCU: National Central University, Taiwan
CWB: Central Weather Bureau, Taiwan,
NTU: National Taiwan University, Taiwan
DPRC, NCKU: Disaster Prevention Research Center, National Cheng Kung University, Taiwan
USP: The University of Shiga Prefecture
KU: Kagoshima University
SU: Shizuoka University
AIST: National Institute of Advanced Industrial Science and Technology

Contact: Norio Matsumoto： n.matsumoto@aist.go.jp 029-861-2380, 3656 (222-42380, 221-33656)

# Seismicity Activation by Strain Rate Change in Iriomote Island, South Ryukyu

Mamoru Nakamura*[1] and Ayumi Kinjou[1]

1. Faculty of Science, University of the Ryukyus, Japan

Among the Yaeyama Islands, south Ryukyu Arc, crustal seismicity has been continuously active in the southwestern part of Iriomote Island. The seismic activity of this part of Iriomote Island abruptly became active in 2002 and 2013. To investigate the cause of this activation, the horizontal crustal strain rate was calculated using the Global Navigation Satellite System (GNSS), and the change of the strain rate was compared with the seismic activity.

For the GNSS data, daily position data of GEONET of the Geospatial Information Authority of Japan were used. The data period was from 1996 to 2017. Long-term (average of 3 years) and short-term (average of 3 months) strain rates in this region were determined using the GNSS data, which were acquired in the islands of Ishigaki, Iriomote, and Hateruma. The results showed that the long-term areal strain rate and the maximum shear strain rate changed in approximately 2002 and in approximately 2013. In the case of 2002, the areal strain rate was dilatational. In the case of 2013, the area strain rate was compressive. Also, the short-term strain rate, which was usually compressional, changed to dilatational approximately every six months. This corresponds to the slow-slip events (SSEs) that have occurred every six months just beneath Iriomote Island.

In addition, the change of seismic activity in the southwestern part of Iriomote Island was detected using the Epidemic-Type Aftershock Sequence (ETAS) model. The hypocenter catalog of the Japan Meteorological Agency was used. The period was from 1998 to 2017. From the secular change of the earthquake detection of the seismic network, earthquakes of M 2.3 or more were used for the analysis. As a result, seismicity activation began around January–April 2002 and around April 2013.

When the activation in 2002 started in Iriomote Island, afterslip in March 2002 occurred in the southern region of Yonaguni Island. The change in strain rate estimated from the afterslip fault model is consistent with the observed strain rate change. In addition, the area in the southwestern region of Iriomote Island, where the seismicity tends to activate, became an area of positive Coulomb failure stress (ΔCFS) as a result of the afterslip. These results suggest that the strain rate change in 2002 was caused by the afterslip.

When the activation in 2013 started, an earthquake swarm, which corresponded to dike intrusion, occurred in the Okinawa Trough at the northern region of Yonaguni Island in April 2013. The strain change caused by the dike intrusion is consistent with the observed strain rate change. In addition, the ΔCFS in the southwestern part of Iriomote Island by the dike intrusion became positive. Therefore, the strain rate change was generated by the dike intrusion in the Okinawa Trough.

These results suggest that the long-term crustal seismicity around Iriomote Island was influenced by the SSEs and the dike intrusion that occurred nearby. This indicates the possibility that underground strain rate changes could be detected and monitored by analyzing seismicity changes.

# M6.7 earthquake off Yamagata prefecture

Yuzo Ishikawa

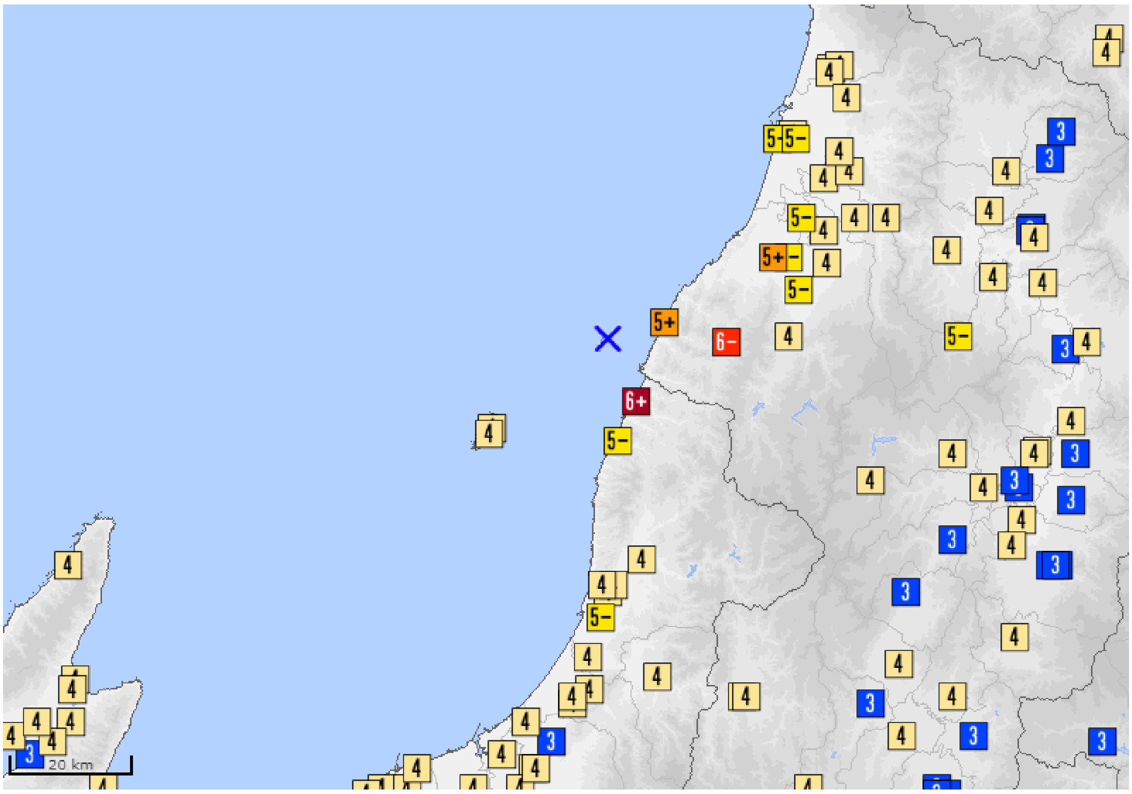


Fig.1; The intensity distribution of M6.7 off Yamagata earthquake.

M6.7(Mw6.5) earthquake occurred off Yamagata prefecture on June 18. The maximum intensity 6strong was recorded at Murakami city, Niigata prefecture. There was no fatality, but 41 persons were injured and nearly 800 houses were damage. The small tsunamis were recorded and the highest one was 11cm at Nezugaseki. The aftershock area is just next to the east of the 1964 M7.5 Niigata earthquake and these events occurred along the new plate boundary of the eastern margin of the Japan Sea in figures 2 and 3. The source fault was estimated as followed by GSI using GNSS data.

| Lon | Lat | top dep | L | W | strike | dip | lake | slip | Mw |
|---|---|---|---|---|---|---|---|---|---|
| 139.378 | 38.574 | 7.6 | 19.7 | 6.2 | 40 | 28 | 99 | 1.2 | 6.4 |

No foreshock was determined by JMA. Only one small earthquake on Aug. 8th was determined before the main shock, but the location of this event was some apart from the area of aftershocks. The activity of aftershocks was not high. The maximum aftershock M4.4 was occurred on Aug. 18. The active period along the new plate boundary will continue more 10 years.

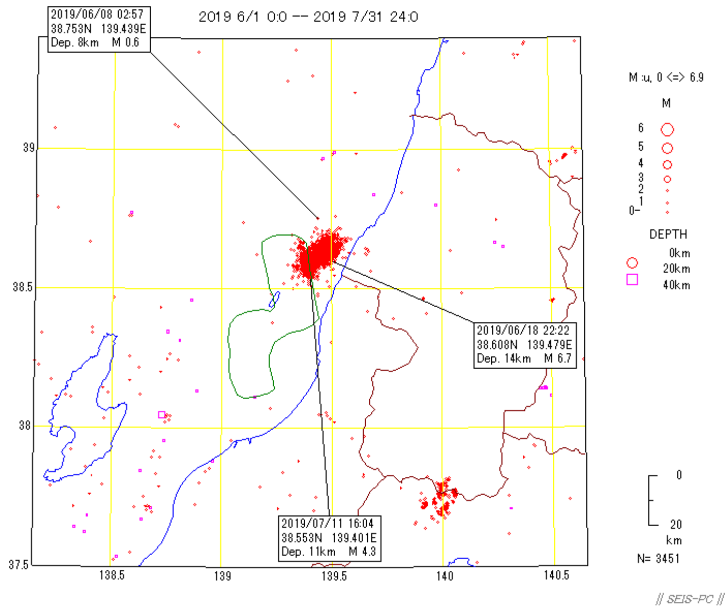


Fig.2: The red marks were the main shock and aftershocks of the M6.7 event. The green line shows the aftershock area of the 1964 M7.5 Niigata earthquake. The parameters of the main shock, M4.3 aftershock and the Aug. 8th were shown.

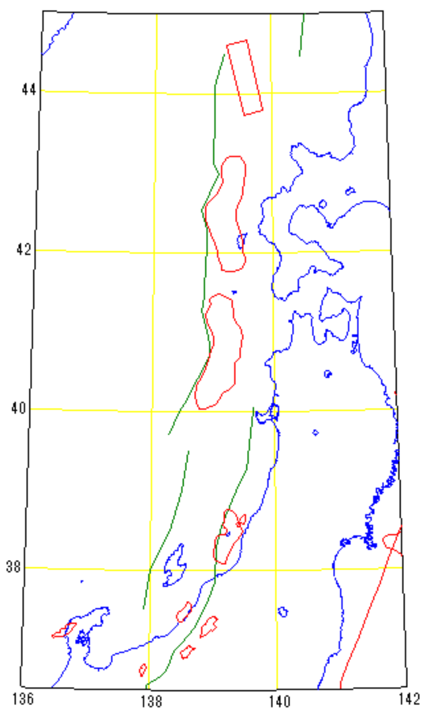

Fig.3: Aftershock areas in red lines except the 1940 M7.5 Off Shakotan earthquake along the new plate boundary in the eastern margin of the Japan Sea. The 1940 event was shown by the fault model for the aftershock area. The green lines show the new plate boundaries.

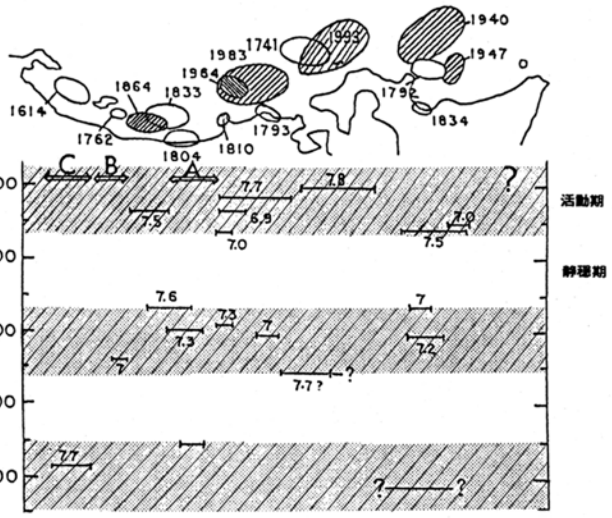


Fig.4: The active periods and the calm period along the eastern margin of the Japan Sea.

# Seismic energy estimation for shallow tremors in the Nankai trough

Suguru Yabe[1], Takashi Tonegawa[2] and Masaru Nakano[2]

[1]National Institute of Advanced Industrial Science and Technology, Japan

[2]Japan Agency for Marine-Earth Science and Technology, Japan

Shallow slow earthquakes have been documented along the Nankai trough. Dense Oceanfloor Network system for Earthquakes and Tsunamis (DONET) has been deployed in the Nankai trough. Shallow tremors and very low frequency earthquakes (VLFEs) in the Nankai trough have been observed with DONET seismometers. Shallow depth of those slow earthquakes may differentiate their characteristics from those of deep slow earthquakes as different depth results in the different tectonic conditions (such as pressure and temperature). We estimated the scaled energy for shallow slow earthquakes and compare it with the scaled energy of deep slow earthquake to understand differences or commonalities between deep and shallow slow earthquakes.

The scaled energy of shallow earthquakes in the Nankai trough is studied in this study. First, we estimated site amplification factors using amplitude of seismic waves from intra-slab earthquakes. We used data from DONET1 and DONET2 stations. Ocean-bottom seismometers usually have 5-10 times larger site amplification than onland seismometers. Then seismic attenuation and seismic energy of events are estimated using signals from shallow tremors. In the Nankai trough, three clusters of shallow tremors are investigated at Off-Kumano region (DONET1), and far off the Kii Channel (around F-node of DONET2) and off the Cape Muroto (around G-node of DONET2). Each cluster has different typical scaled energy. Clusters in off-Kumano region and off the Cape Muroto have the scaled energy at $10^{-9}$-$10^{-8}$, whereas a cluster far off the Kii Channel has the scaled energy at $10^{-10}$-$10^{-9}$. Those values are similar to the scaled energy of deep slow earthquake, which ranges between $10^{-10}$ and $10^{-9}$.

# Evolution of the seismic anisotropy associated with fluid and earthquakes through borehole observation

Kuo-Fong Ma, Ruei-Jiun Hung, Yen-Yu Lin

[1]Earthquake- Disaster & Risk Evaluation and Management (E-DREaM) Center,
National Central University, Taiwan

Through years of observations of TCDPBHS, Taiwan Chelungpu-Fault Drilling Project borehole TCDPBHS, we reveal the temporal variation and evolution of the fault zone anisotropy with local and regional earthquake activities. TCDPBHS is a 7-level three-component vertical borehole seismic array installed in Hole-A of the Taiwan Chelungpu-Fault Drilling Project (TCDP) in July 2006. This array covers a depth range from 946 to 1274 m at intervals of 50–60 m, that crosses the main fault of the 1999 Mw 7.6 Chi-Chi earthquake at a depth of 1111 m. For microseismicity detection from TCDPBHS continuous data, we developed a particle motion template for detections of the events with incident angle less than 30 degree to examine the anisotropy features across the fault. The anisotropy analysis were applied to the coda wave of the identified micro-earthquakes using coda interferometry with stacking through the observation of 2007-2013. We reveal the fault zone with temporal variation in fast shear direction (FSD) as resulted in the observation from anisotropy. We observed variation in FSD within 105-75 degree, and with the stable anisotropy within 8-10% degree in anisotropy through earthquakes, including the effect from fluid (rainfall), and earthquake with large dynamic stress change as observed in peak ground velocity of stations of TCDPBHS. The influence in anisotropy from fluid and earthquakes could increase or decrease the degree of anisotropy, and become to the background values (as within 8-10% degree). These observations suggest that a fault zone could be influenced by fluid and local earthquake, but intend to come back to the background level in stress direction and anisotropy with a recovery period of about 4-6 weeks in average. Through the yearly observation from fault zone in-situ borehole seismometers, we could give a first hand close-in observation of fault zone behavior and its temporal evolution. In view of this temporal observation in an identified fault zone site, we intend to build another geophysical/geochemical borehole observatory in Milun fault, which associated with the 20180206 Hualiean earthquake. The high resolution in-situ fault zone observatory might be able to provide the first hand observation associated with its related fault/subduction zone system for further investigation on the geological features among fluid, earthquake, and fault zone.

# Seismic velocity monitoring using ACROSS on landslide area

*Ryoya Ikuta[1], Kentaro Kodaira[1], Masakiyo Ohishi[2], Takahiro Kunitomo[2] ,
Toshiki Watanabe[2] , Koshun Yamaoka[2] , Akio Katsumata[3]
1. Faculty of Science, Shizuoka University
2. Earth and Volcano Research Center, Graduate school of Environmental Studies, Nagoya University
3. Meteorological Research Institute, Japan meteorological Agency

In this study, we monitored the propagation property of seismic wave and ground deformation on the landslide area using the Accurately Controlled Routinely Operated Signal System (ACROSS) and the extensometer. ACROSS is a seismic source unit which continuously generates precisely controlled seismic wave, which is installed in the Mori-town, Shizuoka prefecture (Fig.1, Fig.2). The purpose of our study is to know how the propagation property of seismic wave changes in response to groundwater level change. We deployed two seismometers on a tea field cultivated on the landslide area (ocha-station) and on a stable land as a reference(ref-station). Seismogram of the two stations were obtained in two periods in two years; from October 2 to October 23 in 2017 and from October 11 to December 26 in 2018.

Figure 1. ACROSS source installed at Mori town. The source generate seismic signal from 3.5 to 7.5 Hz.

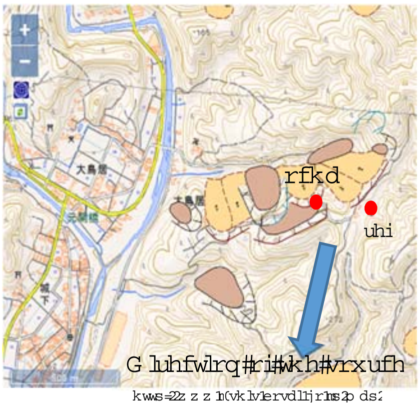


Figure 2. Research site. Two seismometers are deployed around land slide area at 3km distance from the source.

In the transfer functions between the ACROSS source and the seismometers, significant phases are identified as P, S, Love and Rayleigh waves whose traveltimes are around 1.0, 1.8, 2.8 and 3.8 seconds, respectively (Fig.3). Temporal variation of these traveltimes is estimated using a cross correlation procedure. As a result, the traveltimes show significant delay with rainfall and advance during the period without rain.

To compare the traveltime variation with the groundwater level, we estimated the groundwater level by taking convolution between hourly rainfall and exponential decay function of various time constants. According to the correlation between estimated groundwater level and the traveltime variation, the groundwater level modeled with the decay constant of 20 days explains the traveltime changes the best.

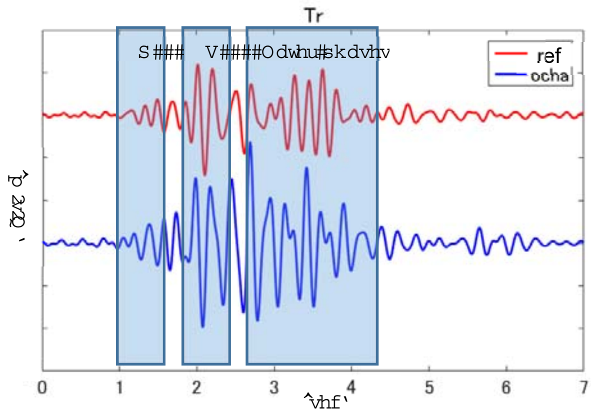


Figure 3. An example of transfer function between ACROSS source and the seismometers. Tr means "T"ransverse component of seismometers with reference to "r"adial direction vibration of the source.

With more detailed analysis, we found that the response of the traveltime to the groundwater is different between Love and Rayleigh waves. The response of the Love wave to the ground water level is linear and more sensitive than that of the Rayleigh wave. On the other hand, the response of the Rayleigh wave shows non-linear response to the ground water level. The traveltime of the Rayleigh wave is more sensitive with higher water level, which changes more rapidly (Fig.4). This can be explained that the groundwater level has two time constants; the Love waves are sensitive to slow pore pressure change in deep area and the Rayleigh waves are sensitive to rapid groundwater flow in shallow area.

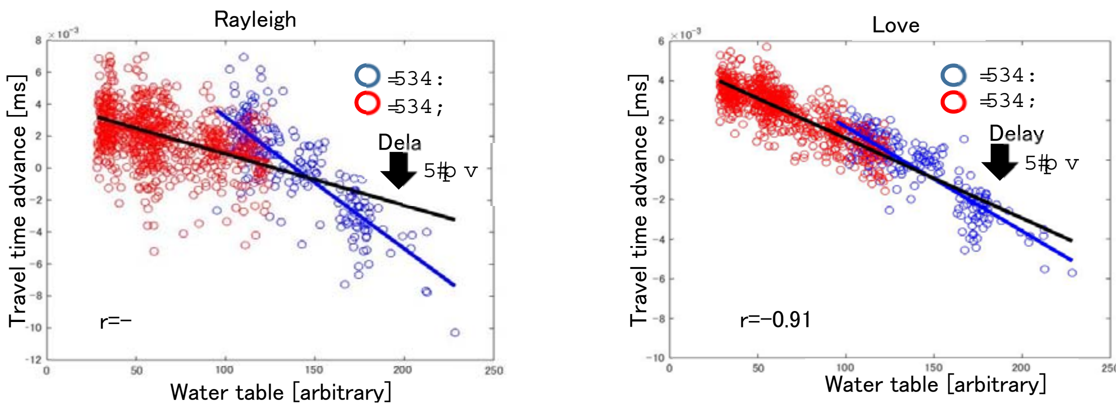


Figure 4. Scatter plot of water level and traveltime advance of Rayleigh wave (left) and Love wave (right). Blue open circles correspond to 2017

To find the local characteristic of the response at the landslide area, we took difference of traveltime change between ocha and ref stations (ocha-ref) and calculated proportionality coefficient and correlation coefficient between the groundwater level and ocha-ref. As a result, high correlations were seen at the arrival times of miner phases than the main phases. Looking at the traveltime changes of these waves, we found that the traveltime changes of the ocha-station corresponds better to rainfall than that of ref-station. Continuous observation of these waves may detect the sign of landslide.

# Assessment of seismic potential in Metropolitan Manila induced by the Marikina Valley fault: Insight from 2019 Castillejobs Mw 6.1 Earthquake

Min-Chien Tsai[1,*], Ying-Hui Yang [2], Mario A. Aurelio[3], John Agustin P. Escudero[3], Jyr-Ching Hu[4]

1. Seismological Center, Central Weather Bureau, Taipei, Taiwan, R.O.C
2. School of Civil Engineering and Architecture, Southwest Petroleum University, Chengdu, China
3. National Institute of Geological Sciences, University of the Philippines, Quezon City, Philippines
4. Department of Geosciences, National Taiwan University, Taipei, Taiwan, R.O.C.

The 2019 Castillejobs earthquake occurred in the Zambales Range of the central Luzon Island in Philippine. However, there is no active fault found around the seismogenic zone according to previous investigations. Here, both the ALOS-2 and Sentinel-1 Synthetic Aperture Radar (SAR) images are collected for mapping the coseismic surface deformation fields of the mainshock. We infer the coseismic faulting model based on the ascending and descending InSAR data of the 2019 Castillejobs earthquake. The best fitting result shows that a fault planar with strike angle of 242.3°, dip angle of 82.2° is responsible for the mainshock. The estimated faulting model suggests that the significant fault slip is concentrated at depths of 0.4-9.5 km and characterized by dominant dextral slip and slight dip slip. And the maximum slip with magnitude of ~0.75 m is located at the depth of ~4.0 km. A slip deficit zone with average slip deficit magnitude ~0.3 m is found from the faulting model, which is corresponding to a moment magnitude of Mw 5.4. In addition, the Coulomb Failure Stress (CFS) change on the Marikina Valley Fault (MVF) due to the fault rupture of the 2019 Castillejobs earthquake is about half of 0.01 bar, which has not significantly changed the CFS status and rupture risk of the Marikina Valley fault, and just advances the occurrence of the earthquake less than 0.5 years in most areas of the MVF. The historical strong earthquakes cause significant CFS drop on the north end of the MVF, which delays the occurrence of the earthquake for ~6.7 years. However, the accumulated positive CFS change causes the occurrence of the earthquake ~6-7 years advancing of schedule in most areas of the MVF. It suggests that the MVF has a high seismic risk in the next 40-50 years.

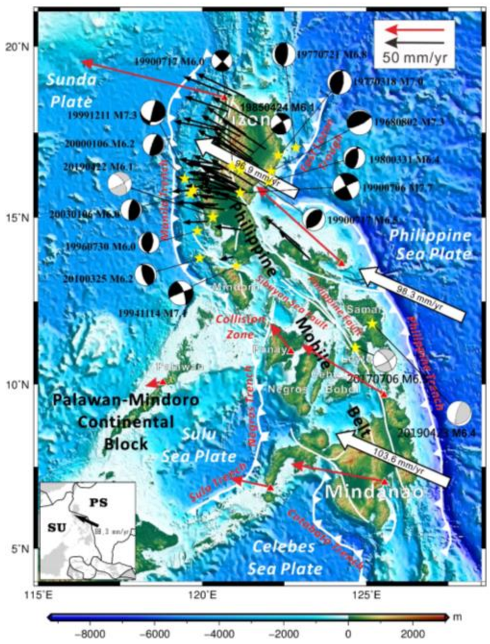


Figure 1 Tectonic background of Philippines. The black arrows indicate the GPS horizontal motion vectors in Luzon Island (Hsu et al., 2016). The red arrows show the NW directed block motion vectors from GEODYnamics of south and SE Asia (Aurelio et al., 1998). The white solid lines are the surface traces of the active faults. The yellow stars indicate the strong earthquakes with magnitude larger than M 6.0.

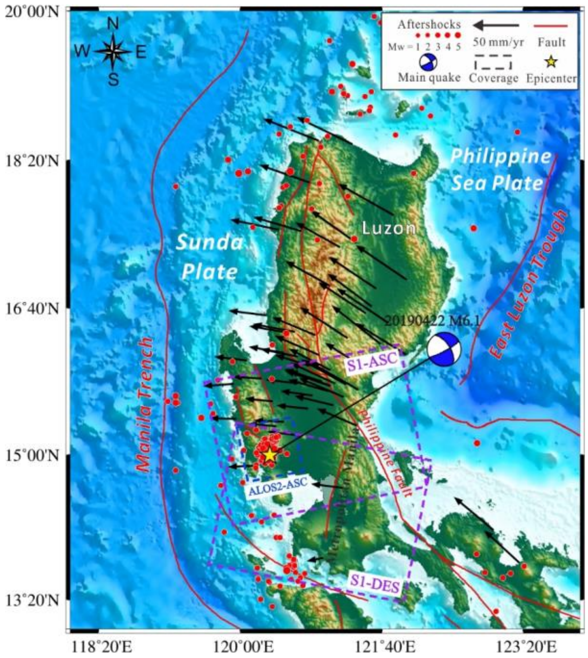


Figure 2 Map of the study zone. Black arrows indicate the GPS horizontal motion vectors. Dashed rectangles denote the coverage of the ALOS-2 and Sentinel-1 SAR images. Red solid lines are the surface trace of the active faults in the Luzon Island. Yellow star indicates the location of the epicenter of the 2019 Castillejobs earthquake, and the red circles represent the aftershocks. The light blue shadow area is the Metropolitan Manila.

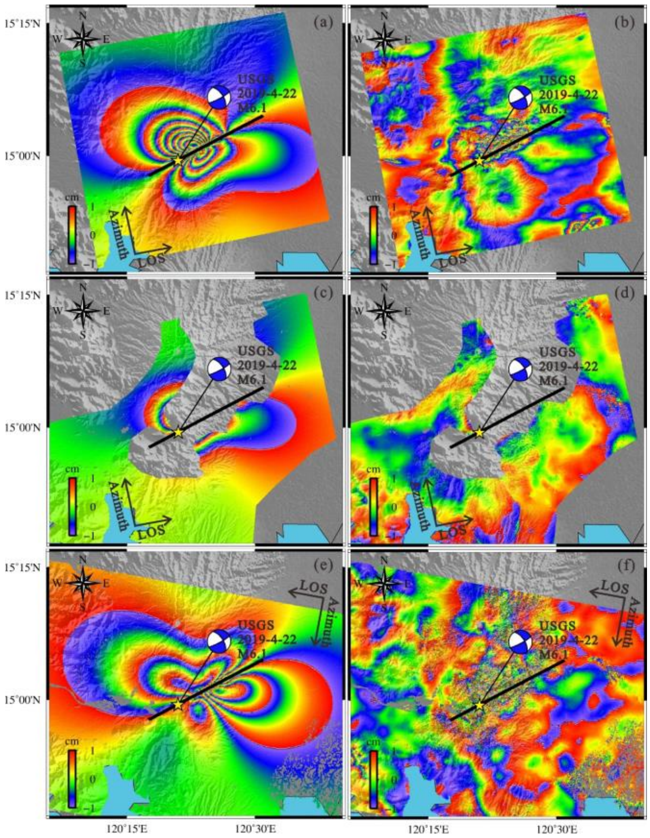

Figure 3 Predicted InSAR deformation fields and residuals between the observations and predictions. Predicted InSAR deformation of the ALOS-2 ascending (a), Sentinel-1 ascending (c) and Sentinel-1 descending (e). Residual fringe distribution of the ALOS-2 ascending (b), Sentinel-1 ascending (d) and Sentinel-1 descending (f). Black solid line indicates the surface trace of the inferred coseismic fault, and the yellow star denotes the epicenter of the 2019 Castillejobs earthquake.

## References

Hsu, Y. J., Yu, S. B., Loveless, J. P., Bacolcol, T., Solidum, R., Luis Jr, A., & Woessner, J. (2016). Interseismic deformation and moment deficit along the Manila subduction zone and the Philippine Fault system. *Journal of Geophysical Research:Solid Earth,* **121**(10), 7639-7665..

Yu, S. B., Hsu, Y. J., Bacolcol, T., Yang, C. C., Tsai, Y. C., & Solidum, R. (2013). Present-day crustal deformation along the Philippine Fault in Luzon, Philippines. *Journal of Asian Earth Sciences*, **65**, 64-74.

# Shallow coseismic slip in a triangle zone of 2019 $M_L$ 6.0 Changning earthquake in Sichuan Basin: Triggering by shale gas hydraulic fracturing?

Jyr-Ching Hu[1,*] and Ying-Hui Yang[2]

1. Department of Geosciences, National Taiwan University, Taipei, Taiwan, ROC
2. School of Civil Engineering and Architecture, Southwest Petroleum University, Chengdu, China

The ALOS-2 and Sentinel-1 satellites synthetic aperture radar (SAR) images are used to investigate the surface deformation and fault rupture of the 2019 $M_L$ 6.0 Changning earthquake occurred in a fold-and-thrust belt in Sichuan Basin, China. Both the ascending and descending interferometric synthetic aperture radar (InSAR) deformation fields (Fig. 1) show that the significant surface deformation is observed on the hanging wall of the seismogenic fault located in a triangle zone in the Changning fold zone, which suggests remarkable fault slip occurred on the coseismic fault in the shallow depth. The preferred faulting model (Fig. 2) suggests that the coseismic rupture occurs on a single planar fault surface with a strike angle of 312.9º, dip angle of 27.6º. And the inferred seismogenic fault has a good consistency with the existed SW-vergence shallow fault in the triangle zone of the Changning anticline (Fig. 3). Two significant slip sources are determined by the geodetic data: one is located within the depth range of 1.8-3.5 km with a peak slip of ~0.7 m, and the other occurs at the shallower depth (0-1.8 km) with a peak slip of ~0.5 m. Previous study suggested that the $M_L$ 5.8 event occurred on 16 December 2018, the ML 5.3 occurred on 3 January 2109 and a sequence of earthquakes in Changning shale gas block were induced by hydraulic fracturing at a depth of ~2.5-3 km. Thus we calculate the Coulomb failure stress transfer caused by the previous two $M_L$ > 5.0 earthquakes, the resulting stress transfer is smaller than 0.1 bar, inferring the possibility of the 2019 M 6.0 Changning earthquake. Moreover, we hypothesize that the hydraulic fracturing of shale gas production in the seismic zone may have a positive triggering effect on the failure of the seismogenic fault of the 2019 M 6.0 Changning earthquake.

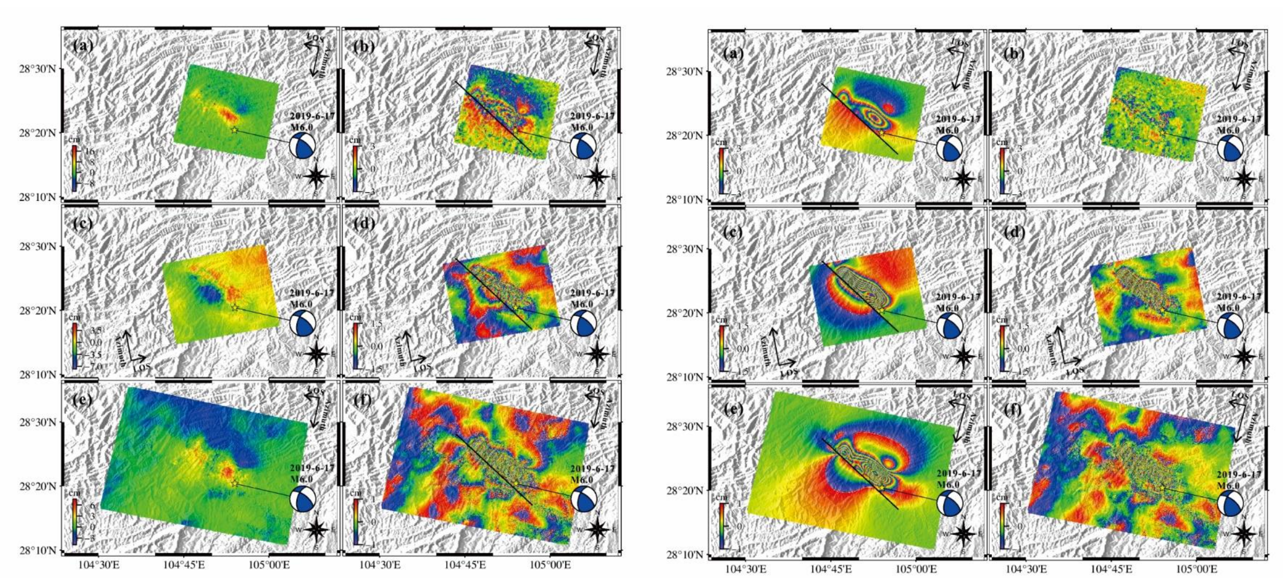


Figure 1. Coseismic deformation from InSAR observation (right panel) and predicted interferograms and residuals (right panel). Both ascending and descending Sentinel-1 and descending ALOS-2 images are used for this study. Focal mechanism of mainshock is form China Earthquake Administration (CEA).

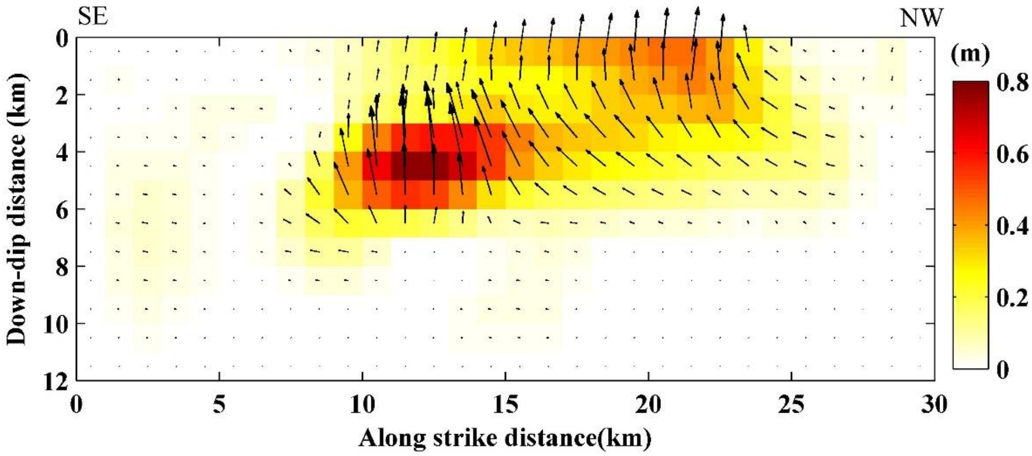


Figure 2. Inferred faulting model of coseismic slip distribution on fault plane from the InSAR deformation fields in Figure 1.

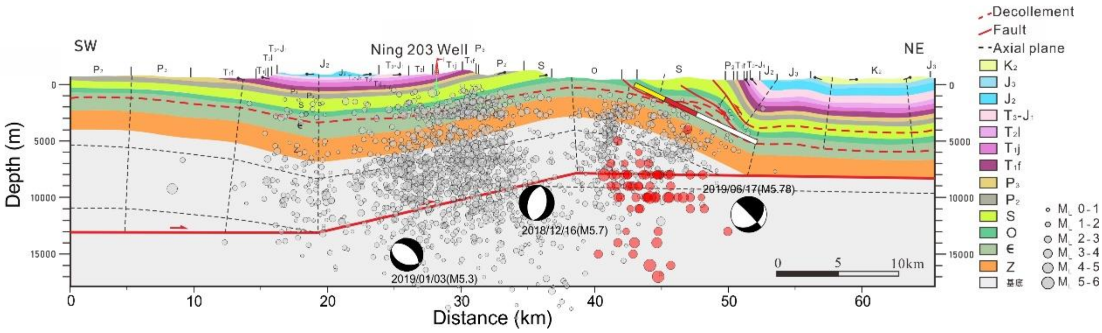


Figure 3. Geologic cross section interpreted from seismic reflection data (Courtesy of Dr. Renqi Lu) Weighted line colored by white (insignificant slip segment), red (peak slip segment) and yellow (significant shallow slip segment) indicate the inferred coseismic fault of the 2019 Changning earthquake. Gray dots are the historical earthquakes in the seismic zone (Data from He et al. 2019), and the red dots denote the aftershocks of the mainshock (Data from USGS and CEA).

## References


He D., R. Lu, H. Huang, X. Wang, H. Jiang, W. Zhang (2019). Tectonic and geological background of the earthquake hazards in Changning shale gas development zone, *Petrol. Explor. Dev.* **46(3)**, in Chinese with English abstract.

Lei, X., S. Ma, W. Chen, C. Pang, J. Zeng, and B. Jiang (2013). A detailed view of the injection-induced seismicity in a natural gas reservoir in Zigong, southwestern Sichuan Basin, China, *J. Geophys. Res.-Solid Earth* **118**, 4296–4311, doi: 10.1002/jgrb.50310.

Lei, X., D. Huang, J. Su, G. Jiang, X. Wang, H. Wang, X. Guo and H. Fu (2017). Fault reactivation and earthquakes with magnitudes of up to Mw4.7induced by shale-gas hydraulic fracturing in Sichuan Basin, China, *Sci. Rep.* **7**, 7971, doi: 10.1038/s41598-017-08557-y.

Lei, X., Z. Wang, and J. Su (2019). The December 2018 $M_L$ 5.7 and January 2019 $M_L$ 5.3 earthquakes in South Sichuan Basin induced by shale gas hydraulic fracturing, *Seismol. Res. Lett.* **90(3)**, 1099-1110, doi: 10.1785/0220190029.

Meng, L., A. McGarr, L. Zhou, and Y. Zang (2019). An investigation of seismicity induced by hydraulic fracturing in the Sichuan Basin of China based on data from a temporary seismic network, *Bull. Seismol. Soc. Am.* **109(1)**, 348–357, doi: 10.1785/0120180310.

# $^{222}$Rn concentration distribution on active faults in Yatsushiro Sea

Kuniyo Kawabata[1], Fumiaki Tsunomori[2], Yujin Kitamura[1] and Hkuho-Maru K 18-3 scientists

[1]*Kagoshima University*, [2]*The University of Tokyo*

Radon concentrations in Yatsushiro sea were surveyed to examine relationship with the submarine sediments and geological structure such as submarine active faults.

Rn-222 is a radioactive noble gas and occurs naturally in earth's crust as an intermediate step in the normal radioactive decay chain of uranium series. Radon shows high solubility for water and thus high mobility through groundwater and fluids in earth's crust. Concentration of radon in groundwater can provide a clue to understand geology of the aquifer and state of crustal deformation as crack formation and change in strain state, because its release rate depends mainly on rock surface area. Recently location of active faults and its activity have been examined by using the method (e.g. Tsunomori et al., 2017).

A bunch of submarine active faults underlies in Yatsushiro area sea. These faults are part of the Futagawa-Hinagu Fault zone which was activated at the 2016 Kumamoto earthquake. R/V Hakuho-Maru sailed for research expedition (KH-1803) in Yatsushiro sea from 27th to 30th July, 2018 to evaluate records of submarine landslides and changes in submarine circumstances due to historical earthquakes. We collected bottom water from obtained multiple cores and piston cores, and pore waters from piston cores for the measurement of the radon concentration in the s eawater on board. The results of radon concentration distribution from multiple cores, (MC 1-12), show that higher concentration along the Line Y18a. The radon concentrations from bottom water of piston cores (PC 1- 11) also show similar results while the values are larger than the results from multiple cores. A higher radon concentration is attributed to difference in (1) radium concentration in sediments, and/or (2) properties of sediments such as porosity and/or surface area of grains which are caused by difference in types of sediment or fault activity in sediments. The Line Y18a extends across a major submarine active fault (FA1, Tanoura-Tsunagi-oki-faults) (Kagohara et al., 2011). Such a geological setting suggests that the radon concentration distribution in Yatsushiro sea might reflect the current fault activity. We discuss the contributing factor of the higher radon concentration by comparison with Ra concentration in sediment, sediment properties in each site and geological structure in Yatsushiro sea.

# Exploring the release of radioactive gas in the volcanic area and its tectonic implications

Ching-Chou Fu[1], Lou-Chuang Lee[1], Tsanyao Frank Yang[2, †], Cheng-Horng Lin[1], Vivek Walia[3], Cheng-Hong Chen[2]

1. Institute of Earth Sciences, Academia Sinica, Taiwan
2. Department of Geosciences, National Taiwan University, Taiwan
3. National Center for Research on Earthquake Engineering, NARL, Taiwan
† Deceased

Key words: radon, gamma ray, subduction zone, pre-seismic activity

Taiwan is tectonically situated in a terrain resulting from the oblique collision between the Philippine Sea plate (PSP) and the Eurasian plate (EP). The continuous observations of gamma rays at the YMSG station and soil radon at the TPT station are recorded in volcanic area and around a major fault zone, respectively, in north Taiwan for the volcanic and seismic studies. A number of anomalous high gamma-ray counts and radon concentrations at certain times can be found. It is noted that significant increase of soil radon concentrations can be observed and followed by the increase in gamma rays a few days to a few weeks before the earthquakes, which occurred in northeastern Taiwan. These earthquakes are usually related to the subduction of PSP beneath EP to the north along the subduction zone in northern Taiwan (e.g., $M_L$=6.4 April 20, 2015). A further comparison of gamma-ray data, local geomagnetic variations and micro-earthquakes in Tatun Volcanic area may imply that the process of local rock fracture for gas and fluid migration, potentially associated with the pre-seismic slow slip. Hence, it is suggested that the pre-seismic activity of an earthquake may be associated with pre-seismic slow geodynamic processes at the subduction interface, leading to the stress of PSP movement to trigger radon enhancements at TPT station. Furthermore, the further movement of PSP may be locked by the EP and accumulated elastic stress results in the increase of gamma rays due to the increase in porosity and fractures below the YMSG station.

# Hydrology Anomalies Triggered by 2016 Taiwan Meinong Earthquake

Shih-Jung Wang[1]*, Yan-Yao Lin[1], Wen-Chi Lai[2], and Hone-Jay Chu[3]

[1]Graduate Institute of Applied Geology, National Central University, No. 300, Zhongda Rd., Zhongli District, Taoyuan City 32001, Taiwan

[2]Disaster Prevention Research Center, [3]Department of Geomatics, National Cheng Kung University, No.1, University Road, Tainan City 70101, Taiwan

*Corresponding author:

Email: sjwang@ncu.edu.tw

Phone: +886-3-4227151 ext. 65870    Fax: +886-3-4263127

## Abstract

Using the observed hydrologic anomalies to investigate the earthquake induced hydrogeological variations can help us realize the effect on the regional water cycle and groundwater resource. The hourly and secondly data of groundwater level variations and the hourly river discharge variations triggered by the Taiwan Meinong earthquake are checked and analyzed to investigate the responses under different hydrogeological conditions in west and south regions of epicenter. At the same location, the groundwater level change before and after the earthquake show an increase for shallow aquifer and a decrease for deep one. This phenomenon expresses that groundwater flows from a high pore water pressure in the deep depth to a low pore water pressure in the shallow depth due to a developed flow path created by the Meinong Earthquake. This phenomenon cannot be described using the traditional poroelastic model under the effective stress concept. The developed flow path might relate to a surface fracture caused by the Meinong Earthquake since the wells shown this phenomenon are located near the fracture area. Increased river discharges are also observed near the fracture area. The additional surface water must come from groundwater discharge and it is consistent with the surface fracture and the upward groundwater flow. The increased groundwater levels are shown to consistent with the horizontal peak ground velocity (PGV), which imply that the increased groundwater levels might result from the buildup pore water pressure induced by shear strain, like the liquefaction mechanism. Therefore, the step groundwater level variations do not show good relationship with epicentral distance. Besides, the observation of step groundwater level variations shows better agreement by using epicenter #2 than epicenter #1, which is proposed in literature. The Meinong Earthquake slightly influences river hydrology but largely influence groundwater hydrology in both spatial and temporal domains in the western part of epicenter. The main factors can be seismic energy propagation, hydrogeological properties, and the confinement, though they are dependent. The study results provide different point of view to explain the hydrologic anomalies induced by earthquakes that can be used to assess how earthquakes influence the water cycle and resource.

**Keywords**: Groundwater level, River discharge, Hydrogeology variation, Taiwan Meinong earthquake.

# Postseismic hydrological changes associated with the 2016 Kumamoto earthquake

*N. Koizumi[1], S. Minote[2], T. Tanaka[3], A. Mori[4], T. Ajiki[5], T. Sato[6], H. A Takahashi[6], and N. Matsumoto[6]

1. School of Environmental Science, the University of Shiga Prefecture,
2. Taneya Co.Ltd.,
3. JA Lake Otsu,
4. Yodogawa Hu-Tech Co., Ltd.
5. Kinki Eco Science Inc.,
6. AIST, Geological Survey of Japan, Research Institute Earthquake and Volcano Geology

The 2016 Kumamoto earthquake, whose main shock was M7.3 event on April 16, 2016 28 hours after the foreshock of M6.5, caused severe damage in and around Kumamoto Prefecture, Japan. It also caused postseismic hydrological changes in Kumamoto Prefecture. In this study, we analyzed daily streamflow data collected by eight observation stations from 2001 to 2017 in regions that experienced strong ground motion during the 2016 Kumamoto earthquake. We also surveyed 11 spring waters in the regions several times after the main shock. Streamflow did not increase immediately following the earthquake; however, increases were recorded at some of the eight stations following a heavy rainfall that occurred 2 months after the earthquake. A decrease in the water-holding capacity of the catchment caused by earthquake-induced landslides can explain this delayed streamflow increases. On the other hand, the spring flow rate did not show so clear earthquake-related changes. Water temperature and chemical composition of spring waters were also hardly changed. Only the concentration of $NO_3^-$, which is usually considered to be supplied from surface, somewhat changed just after the earthquake. These results show that the postseismic hydrologcical changes were caused mainly by earthquake-induced surface phenomena and that there was little contribution of deep seated fluid.

# The study of the mechanism of earthquake-induced groundwater changes in Taiwan: An update in recent earthquakes.

Wen-Chi LAI[1*], Shih-Jung WANG[2], Norio Matsumoto[3], Naoji Koizumi[4]

[1]*National Cheng Kung University, Taiwan*

[2]*National Central University, Taiwan*

[3]*AIST, Geological Survey of Japan, Institute of Earthquake and Volcano Geology*

[4]*School of Environmental Science, the University of Shiga Prefecture*

[*]*Corresponding author: laiwenji@dprc.ncku.edu.tw* [+]*Presenter*

## Abstract

The earthquake-induced groundwater level changes were recorded in many historical records. Such changes have been monitored and investigated in the last fifty years. However, most of the previous studies, which are based on single event in different observations or multiple-independent events by many different data sources, involved uncertainties arising from different mechanisms and site effects. The quantitative analysis of earthquake-induced groundwater level changes remains a challenge. In this study, the datum of Taiwan Groundwater Monitoring Network induced by disastrous earthquakes ($M_W \geq 6.0$) in recent 20 years 2008 ~ 2018 were utilized. The previously strain sensitivities of the groundwater level at those wells ranged between 1 ~ 5 mm/$10^{-8}$, indicating that an analysis of groundwater level data at these wells can detect volumetric strain changes on the order of $10^{-8}$. A total of 27 events had been examined to explore the mechanism of the earthquake-induced groundwater variation. Earthquake-related groundwater level changes were compared to observed seismic accelerations and to infer coseismic static volumetric strain changes at the wells. The strain to cause the groundwater variation composes two parts: static strain and dynamic strain. The static volumetric strain is caused due to the presence of inhomogeneous structures of tectonic structures and well-aquifer system, which the dynamic strain is mainly caused by ground shaking.

On the whole, ground shaking seems a dominant factor for the earthquake-related changes at the most of wells in alluvial layers because the calculated static volumetric strain is far less than the observed strain that corresponds to the earthquake-induced groundwater variation. The analysis shows that the acceleration of ground shaking cannot always fits to the observed groundwater level changes.

# Changes in groundwater pressure associated with the 2018 Osaka Hokubu earthquake (M6.1) at the Takarazuka observatory

Norio Matsumoto and Tsutomu Kiguchi
*Geological Survey of Japan, AIST*

## Abstract

We observed a large anomalous change in groundwater pressure at TKZ associated with the 2018 Osaka Hokubu earthquake ($M_{jma}$ 6.1) occurred in 18 June 2018. TKZ observatory is located 26 km west of the epicenter. Groundwater pressure decreased 14 cm just after the earthquake, and then it suddenly increased. Total increase of the groundwater pressure was 4.65 m at TKZ seventeen days after the earthquake.

After 2000, we observed eight postseismic changes in groundwater pressure more than 10 cm at TKZ. Six of the eight postseismic changes were caused by all earthquakes whose JMA seismic intensity scale were more than 3 at TKZ. Other two were caused by earthquakes whose JMA seismic intensity scale were 2 at TKZ.

In particular, three postseismic changes in groundwater pressure associated with the 2000 Tottori Seibu earthquake, the 2011 Tohoku-oki earthquake and the 2018 Osaka Hokubu earthquake were more than 1 m. Normalized curves of the there groundwater-pressure curves after the earthquakes are similar to each other.

These postseismic changes in groundwater pressure are not caused by sudden increase of groundwater pressure near TKZ, because hydraulic conductivity (permeability) of the well in TKZ is 2.3～3.5 x $10^{-8}$ m/s (2.3～3.5 x $10^{-15}$ $m^2$) and groundwater-pressure increase at TKZ should finish less than one day if we have sudden increase in groundwater pressure near the well.